Journal of Solid State Chemistry 182 (2009) 1082–1087

Contents lists available at ScienceDirect

Journal of Solid State Chemistry

journal homepage: www.elsevier.com/locate/jssc

Formation of calcium carbonate films on chitosan substrates in the presence of polyacrylic acid

Linghao He [a], Rui Xue [a], Rui Song [a,b,*]

[a] Zhengzhou University of Light Industry Henan Provincial Key Laboratory of Surface and Interface Science, Henan, Zhengzhou 450002, China
[b] College of Chemistry and Chemical Engineering, Graduate University of Chinese Academy of Sciences, Beijing 100049, China

ARTICLE INFO

Article history:
Received 5 December 2007
Received in revised form
21 March 2008
Accepted 24 March 2008
Available online 27 March 2008

Keywords:
Chitosan
Calcium carbonate
Polyacrylic acid

ABSTRACT

In this investigation, chitosan membranes with different surface average degrees of deacetylation (DA) are prepared and then are employed as the support matrix to culture calcium carbonate ($CaCO_3$). In the presence of high concentration of polyacrylic acid (PAA), the $CaCO_3$ films obtained on the surface of all chitosan films mainly consisted of vaterite, which suggests the presence of bulk PAA plays an overwhelming part in stabilizing the vaterite. As a comparison, the influences of active groups indicate that only in case of low concentration PAA the thin $CaCO_3$ films grown on chitosan with 8% DA mainly consisted of vaterite owing to the strong nucleation ability of $-NH_2$ group, whereas, for those grown on chitosan with 80% DA the $CaCO_3$ films mainly consisted of aragonite. A more complex scenario revealed that in the case of intermediate concentration of PAA the formed polymorphs behave as mixtures of vaterite and aragonite.

1. Introduction

Biomineralization has recently received much attention from materials scientists, since these biomaterials form inorganic–organic hybrid composites which possess controlled hierarchical structure and show significant properties [1]. In this regard, the nacre of shells is an attractive target for the design of inorganic–organic hybrid materials by mimicking biomineralization processes. It forms a layered structure of brick (formed by calcium carbonate ($CaCO_3$) crystal) and mortar (formed by organic bio-macromolecules), which results in the formation of composites with high mechanical strength and unusual optical properties, such as pearl luster [2].

Materials with layered structures, such as the most widely investigated $CaCO_3$-organic layered materials, are in recent years prepared mainly through the crystallization of inorganic compounds on solid insoluble organic matrixes [3–14]. As reported, $CaCO_3$ can exist in six different forms, of which three major polymorphs are in order of decreasing stability as follows: calcite, aragonite, and vaterite. Two hydrated crystalline forms and an amorphous form of $CaCO_3$ also exist, but they are generally unstable and thus are readily transformed into the calcite, aragonite, or vaterite polymorphs [3,15]. The formation of layered structures depends on the interactions between insoluble organic matrixes, which are used as substrates, and soluble organic matrixes, which can promote heterogenerous nucleation and suppress homogenerous nucleation. Natural organic materials such as cellulose [4], chitosan [3–8], chitin [8]; synthetic organic macromolecules such as polyvinyl alcohol [9], nylon 66 [10], polydiacetylene [11,12]; and even modified polymers such as polymethyl methacrylate [13] were used as solid insoluble organic matrixes. Some acidic macromolecules, such as polyacrylic acid (PAA) [3–9] and polylysine [14] were used as soluble organic matrixes.

As one of the in-depth investigated solid insoluble organic matrixes, chitosan is a cationic biopolymer possessing hydroxyl group (OH) and primary amine (NH_2) groups that become protonated (NH_3^+) in acidic environment. PAA is one of the common soluble additives possessing carboxylate (COOH) groups. Adsorption of PAA on the chitosan matrix can be interpreted as a polyelectrolyte complex, which is influenced by concentrations of PAA remarkably [5]. Just by this action, $CaCO_3$ could be initiated for heterogeneous nucleation on chitosan surface.

Formation of $CaCO_3$ films on the surface of chitosan membranes is attributed to the direct growth of a mineral phase from a supersaturation solution with PAA. To date, many studies have focused on the influential variables including temperature [6], molecular weight of PAA [6,7], concentration [7,8] and functional groups [8]. Wada et al. found that films comprised of aragonite and vaterite were formed on chitosan films in the presence of PAA,

* Corresponding author at: College of Chemistry and Chemical Engineering, Graduate University of Chinese Academy of Sciences, Beijing 100049, China. Fax: +86 10 8825 6092.
E-mail address: rsong@gucas.ac.cn (R. Song).

0022-4596/$ - see front matter © 2009 Elsevier Inc. All rights reserved.
doi:10.1016/j.jssc.2008.03.022

with the aragonite {110} plane being partially oriented parallel to the chitosan surface and the vaterite {100} and {110} planes parallel to the chitosan surface [7]. Nevertheless, the relations between the ultimate polymorphs and active groups of chitosan were not considered. In summary, little is known about the dependence of the final mineral phase on the concentration of PAA and main active groups of chitosan films.

In this investigation, chitosan films with low degree of acetylation (DA) are prepared and then they are further acetylated in order to obtain the chitosan films with relatively high DA. The effects of functional groups on crystal phase, as well as the co-influence of concentration of PAA are discussed.

2. Experimental

2.1. Materials

Chitosan with a degree of acetylation of 8% was received from Shanghai Reagent Company, China. Polyacrylic acid (PAA) with Mw of ca. 2.0×10^3 is purchased from Sigma Chemical Co. All the inorganic reagents in this experiment are of analytical grade and are used as received. Ultrapure water (resistance = 18.8 MΩ) is used throughout the experiment.

2.2. Preparation of chitosan film

Chitosan was dissolved in 2% V/V aqueous acetic acid solution at a concentration of 2 wt%. Films were obtained by casting solution on a glass dish and allowing the solvent to evaporate at ~40 °C. Annealing was processed at ~120 °C for 1 h in order to remove the excess water and solvent in the resultant films.

2.3. Acetylation of chitosan film

Chitosan films without annealing were reacted with acetic anhydride in methanol. The ratio of anhydride to methanol in mixture reaction solution was 3:1. Prior to reaction, chitosan film was soaked int methanol for 2 days. After that, chitosan films were taken out from the methanol and dipped into mixture reaction solution for 30 min. Acetylation reaction was terminated by removal of the films from the reaction solution and washing the films over a 15-min time period with five 100 mL of methanol. The films were then dried (120 °C, 1 h) prior to characterizations.

2.4. Preparation of $CaCO_3$ crystals

$CaCO_3$ crystallization was achieved by the diffusion (about 7 h) of NH_3 and CO_2 vapors from solid $(NH_4)_2CO_4$ in a closed box (diameter: 14.0 cm) containing the vessels (diameter: 3.5 cm) with $CaCl_2$ (10.0 mM, 200 mL) and PAA solutions. The chitosan membranes were placed in the vessel containing the $CaCl_2$ solution. $(NH_4)_2CO_3$ powder (1.0 g) was placed in a vial (diameter: 2.7 cm). The diffusion was preformed through the three holes (diameter: 1 mm) in the lid of the vial. Because the whole processes were very sensitive to the diffusion rate of NH_3 and CO_2 from $(NH_4)_2CO_3$, the whole experimental system was kept under thermostatic conditions at ~30 °C for approximately 11 h.

2.5. Characterization

Attenuation total reflection-infrared spectra (ATR-IR, Tensor 27, Bruker Corp.) were used to probe surface chemical character and evaluate the degree of deacetylation of chitosan in films. For all measurements, the spectra were collected with 32 scans at a resolution of 2 cm^{-1} interval. An optical microscope (OM, E600POL, Nikon) was used to acquire the morphology of the samples.

The evaluation of degree of acetylation (DA) was obtained by the relative intensity of characteristic absorption peak [16,17]. According to a previous report, A_{1650}/A_{2877} is one of the best absorbance ratios to accurately determine the degree of deacetylation of chitosan by FTIR spectroscopy, i.e. the C–H stretching at 2877 cm^{-1} was used as a reference band, since the intensity of this band did not change with the DA. Meanwhile, amide I band at 1650 cm^{-1} was used as a probe band [17]. The baselines were selected as shown in Fig. 1. The DA of chitosan used in our experiment was equal to ca. 8%, and then the following formula could be used to evaluate the approximate degree of acetylation of acetylated chitosan film (DA_B):

$$8\%/(A_{1650}/A_{2877})_A = DA_B/(A_{1650}/A_{2877})_B \quad (1)$$

3. Results and discussion

3.1. Modification of chitosan film

The chemical moieties of chitosan films (A) and acetylated chitosan films (B) are evaluated with ATR-IR measurement. In the

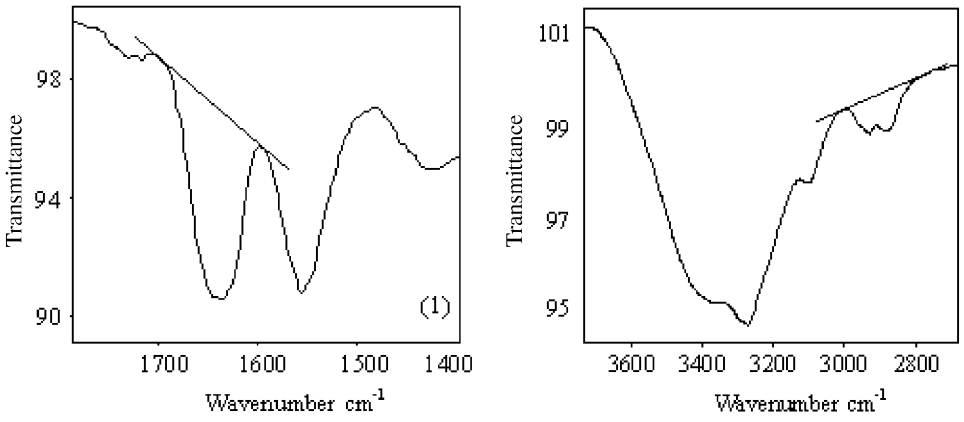

Fig. 1. The selected baselines of absorption at 1650 cm^{-1} (1) and 2877 cm^{-1} (2) in IR spectrum for evaluating the surface average degree of acetylation of chitosan membranes.

ATR-IR spectra of chitosan with 8% DA (Fig. 2A), the absorption peaks at ca. 1650 and 1590 cm^{-1} are assigned to the carbonyl stretching of secondary amides (amide I band) and –NH bending vibrations of non-acetylated 2-amino glucose primary amines, respectively [18]. Upon being acetylated, the increase in adsorption intensity of 1310 cm^{-1} (assigned to the amide III band) and the red-shift of the adsorption peak of 1590 cm^{-1} (–NH bending vibrations of amide II band, shift from 1590 to 1555 cm^{-1}) confirm that a large number of $–NH_2$ groups have been acetylated into amide (Fig. 2B). The appearance of the weak peak at 1735 cm^{-1} indicates that a small section of –OH has been acetylated into ester [18]. Moreover, $–CH_3$ symmetrical bending vibrations at 1376 and 946 cm^{-1} are reinforced compared with the as-received chitosan, implying the high average degree of acetylation.

The surface average degree of acetylation of chitosan membrane after acetylation is estimated to be around 80% according to formula (1). Thus two kinds of chitosan membranes with different active groups are obtained.

Fig. 2. ATR-infra spectrum of chitosan films (A) and acetylated-chitosan films (B).

3.2. Thin-film formation of $CaCO_3$

Essentially, $CaCO_3$ is precipitated on chitosan matrix from its supersaturated solution containing PAA soluble additive. The concentration of PAA in solution plays a key role in precipitating $CaCO_3$. As previously reported, excess or very low concentration of PAA would lead to discontinuous $CaCO_3$ when grown on chitosan matrix, in that very low concentration of PAA usually lacks action with the surface of chitosan, while excess PAA would generate stronger inhibition to grow $CaCO_3$ crystal [8]. Only in the range of suitable concentrations of PAA, a continuous $CaCO_3$ film would be obtained on chitosan matrix, and the interactions among chitosan, PAA and $CaCO_3$ would be present, which lead to the ultimate polymorphs. Thus, in this case, a suitable range of PAA concentration is selected in order to get more insights on the nucleation mechanism of $CaCO_3$ on the surface of chitosan film.

3.2.1. Thin-film formation of $CaCO_3$ on chitosan substrate films

In the range of selected concentrations of PAA, $CaCO_3$ films are developed on chitosan films as shown in Fig. 3. Some connected spherulites with cross lines are observed under a polarized optical microscope, and at least two kinds of spherulites can be found on chitosan membranes with the decreasing concentration of PPA. According to the analysis of ATR-IR results (Fig. 4), we can see the absorption at ca. 875 and 745 cm^{-1}, both ascribed to vaterite [19,20], and the peak at ca. 857 cm^{-1}, which is the characteristic absorption of aragonite [21]; hence, the main polymorph of $CaCO_3$ films developed on chitosan membranes is vaterite, whereas a small amount of aragonite is formed in the case of mid-concentration range of PAA.

3.2.2. Thin-film formation of $CaCO_3$ on modified chitosan substrate films

With increasing concentration of PAA, the morphology and the corresponding ATR-IR data on the evolution of $CaCO_3$ polymorphs developed on the acetylated chitosan membranes are shown in Fig. 5 and Fig. 6, respectively. The results from the polarized optical microscope display a transformation from one to another polymorph. Meanwhile, ATR-IR results confirm the transformation

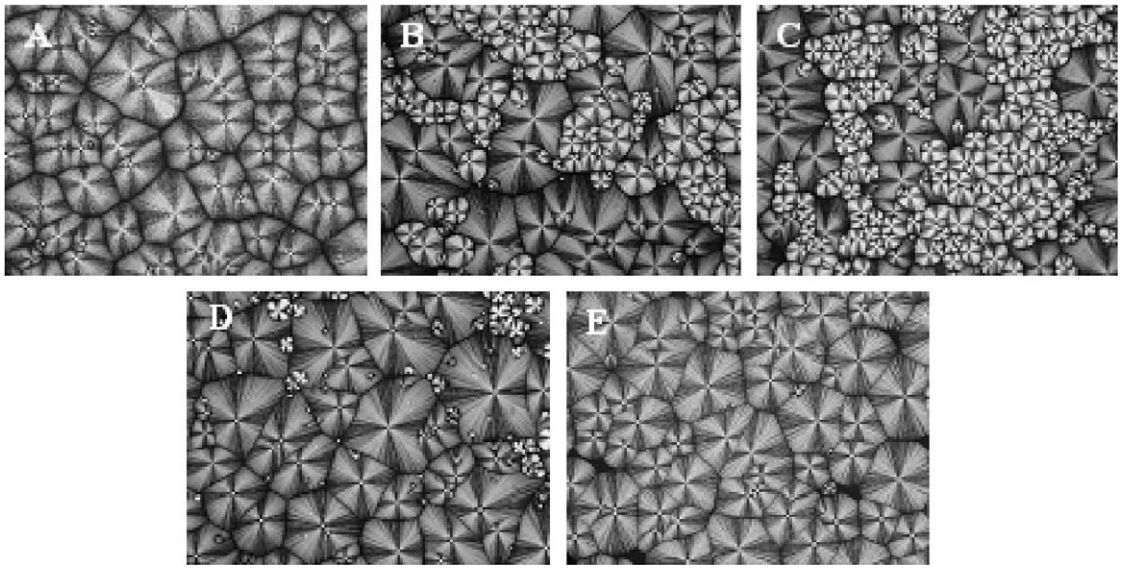

Fig. 3. Polarized optical microscopes of calcium carbonate films developed on chitosan films in the presence of PAA: (A) 1×10^{-3} g/L; (B) 5×10^{-3} g/L; (C) 1×10^{-2} g/L; (D) 5×10^{-2} g/L; (E) 1×10^{-1} g/L.

mainly by the variations in the peaks between 700 and 900 cm^{-1}. In other words, the recession of the peak at 857 cm^{-1} with a concomitant growth of peaks at 875 and 745 cm^{-1} confirm the transformation from aragonite to vaterite.

3.2.3. Comparison

The polymorphic evolutions of $CaCO_3$ developed on surfaces of chitosan and acetylated chitosan films are comparatively displayed in Fig. 7. In the low concentration of PAA, the thin films grown on chitosan with 8% DA mostly consist of vaterite, while those grown on chitosan with 80% DA mainly consist of aragonite, suggesting that DA (main active groups) plays an important part in low concentration PAA. On the contrary, in the presence of PAA with high concentration ($>1\times10^{-2}$ g/L), the thin $CaCO_3$ films grown on chitosan with 8% or 80% DA will mainly consist of vaterite, indicating that the concentration of PAA becomes a dominant factor in high concentration PAA.

The pH value is a characteristic parameter of solution state, which could reflect the mineralization process. The pH variation in the whole mineralization process is shown in Fig. 8. The processes are similar to each other, with the only difference in the initial pH value in the presence of PAA with different concentrations. As the crystallization proceeds, the pH of the solution rapidly increases at early stage, and after 30 min the pH value levels off to a plateau at ca. 9. This pH value is consistent with an ammonium/ammonium hydroxide buffer solution caused by the absorption of ammonia [22]. After reaching this plateau, the pH value is almost constant until the mineralization is terminated, suggesting a stable growth environment of $CaCO_3$. The variation in pH value, especially in the initial stage, indicates different nucleating conditions and is crucial to the ultimate polymorphs. Since various $CaCO_3$ polymorphs are obtained on the surfaces of virgin and modified chitosan films, it could be concluded that the surface chemical character of chitosan film, such as the active groups, will play a key role in inducing the nucleation of $CaCO_3$ mineral phase, especially in the early step of this process.

On the basis of previous studies, in low concentration of PAA, the formation of $CaCO_3$ on chitosan should be equalized by the interplay of two parallel phenomena [7]: (1) firstly, PAA-Ca^{2+} polyelectrolyte composites form in the $CaCl_2$ solution, then the electrostatic force between the $-COO^-$ and the $-NH_3^+$ groups, and moreover, the hydrogen bond between –COOH and –OH, $-NH_2$ groups on the chitosan membrane surface, will lead to the local high supersaturation with $CaCO_3$ around the membrane when CO_2 is diffused into the $CaCl_2$ solution; (2) PAA remains as mobile carboxylic anions in the form of PAA-Ca^{2+} in the $CaCO_3$ solution, and thus inhibits the growth of the island crystals in the $CaCO_3$ solution by its adsorption. The combination of these phenomena will result in a high supersaturation with $CaCO_3$ in the chitosan membrane vicinity, which causes the kinetically controlled condition for crystallization and therefore leads to the formation of $CaCO_3$ island crystals. In this case, the main nucleating groups are $-NH_2$ and –OH on the surface of chitosan with 8% DA as opposed to solely –OH group on the surface of chitosan with 80% DA. As indicated in Fig. 7, for low-concentration PAA system, a large quantity of aragonite would grow on the surface of chitosan rich in –OH, while vaterite is found to grow on the surface of chitosan comprised of $-NH_2$ and –OH. Then, it could be deduced that $-NH_2$ is a stronger nucleating group than –OH, and thus the formation of vaterite was favored. Obviously, the mechanism

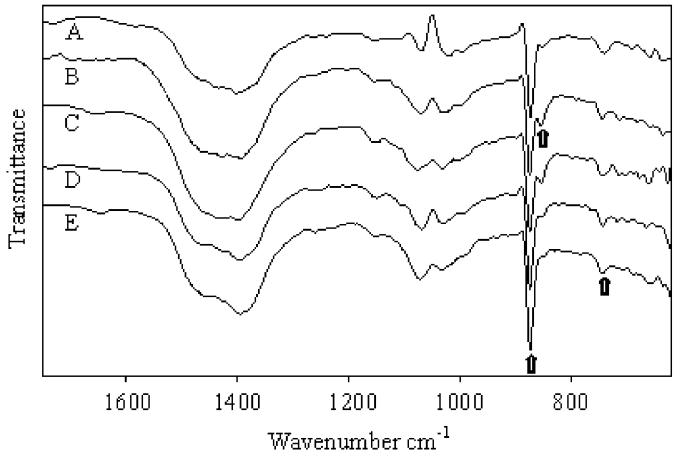

Fig. 4. ATR-infra spectrum of calcium carbonate films developed on chitosan films in the presence of PAA: (A) 1×10^{-3} g/L; (B) 5×10^{-3} g/L; (C) 1×10^{-2} g/L; (D) 5×10^{-2} g/L; (E) 1×10^{-1} g/L.

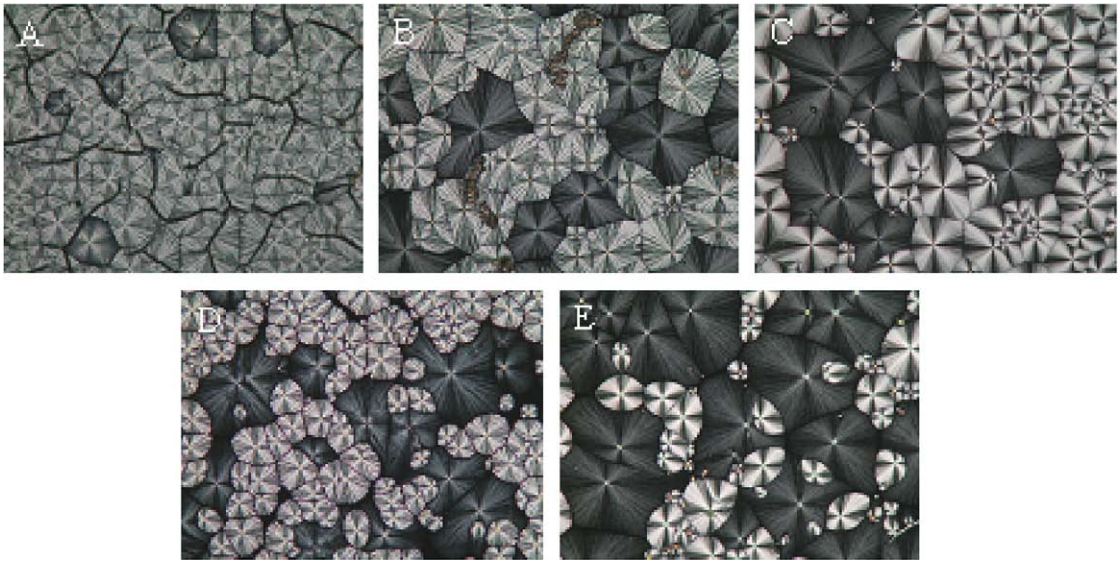

Fig. 5. Polarized optical microscopes of calcium carbonate films developed on chitosan films in the presence of PAA: (A) 1×10^{-3} g/L; (B) 5×10^{-3} g/L; (C) 1×10^{-2} g/L; (D) 5×10^{-2} g/L; (E) 1×10^{-1} g/L.

behind this observation is closely related to the coordinating action between $-NH_2$ and Ca^{2+}. This aspect still deserves further confirmation.

In the case of high concentration of PAA, $-NH_2$ groups will be transformed into $-NH_3^+$ groups [5], which are covered by PAA molecules due to the electrostatic force. At this point, a large number of mobile PAA molecules in the form of PAA-Ca^{2+} exist in the $CaCO_3$ solution [7]. The coverage of PAA over the whole chitosan film would make the active groups out of action. As a result, the PAA molecules absorbed on chitosan film should inhibit the growth of the island crystals in the same way as the mobile PAA molecules in the $CaCO_3$ solution. When CO_2 and NH_3 are diffused into $CaCl_2$ solution and the saturation degree of solution increases further, a large number of amorphous $CaCO_3$ enclosed by PAA are firstly formed mainly in body solution, and subsequently moved and absorbed on the surface of chitosan. By this way, the amorphous $CaCO_3$ is eventually transformed into relatively stable vaterite. In the current case, as well indicated in Fig. 8, vaterite is obtained on both chitosan surfaces with 8% and 80% DA, suggesting that the formation of vaterite is due to the stabilization of high concentration PAA.

Based on the discussion above, the co-existence of aragonite and vaterite on chitosan with 80% DA in the presence of mid-concentration PAA becomes understandable, but we still cannot clarify the formation of a small amount of aragonite on chitosan membrane with 8% DA. Assumedly, this result is caused by a competition between active nucleating groups, and the possible mechanism is schematically given in Fig. 9. In the presence of PAA with low concentration, $-NH_2$ and $-OH$ groups are abundant on the surface of chitosan. The stronger nucleating activity of $-NH_2$, as confirmed above, will promote vaterite formation. However, on increasing the concentration of PAA, the amount of $-NH_3^+$ increases, which eventually is covered by PAA molecules and thus loses nucleating activity. Then, the nucleating action of $-OH$ is initiated and a small number of aragonite crystals are induced. With more PAA addition, vaterite crystal is generated since most mobile PAA molecules still remain in the $CaCO_3$ solution.

4. Conclusion

Biomineralization process indicates a profound dependence on polymeric support. Chitosan membranes with 8% and 80% DA display different mineralization properties. In the presence of polyacrylic acid (PAA), thin films grown on chitosan with 8% DA always consisted of vaterite. As a comparison, for chitosan with 80% DA, vaterite crystals only prevail in high concentration of PAA, while aragonite is the main crystal phase in low concentration of PAA. This observation is due to the formation of calcium carbonate ($CaCO_3$), which is influenced synergistically by at least three variables, i.e. concentrations of PAA, $-OH$ and $-NH_2$ groups. In the presence of high concentration of PAA, vaterite would be the dominant phase. However, in low concentration of PAA, the formation of vaterite is ascribed to the strong action of $-NH_2$ on chitosan, while the formation of aragonite is derived from the action of $-OH$. In other words, $-NH_2$ displays stronger nucleating activity than $-OH$, and $-NH_2$ is prone to loss activity due to the over-covering of PAA molecules.

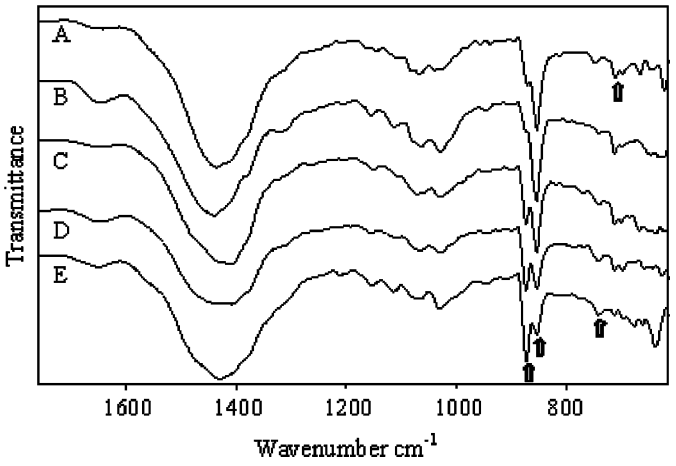

Fig. 6. ATR-infra spectrum of calcium carbonate films developed on acetyl-chitosan films in the presence of PAA: (A) 1×10^{-3} g/L; (B) 5×10^{-3} g/L; (C) 1×10^{-2} g/L; (D) 5×10^{-2} g/L; (E) 1×10^{-1} g/L.

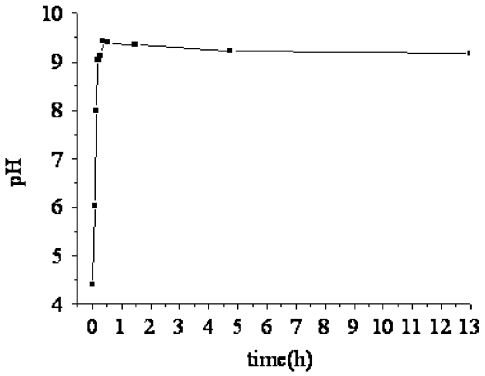

Fig. 8. Plot of pH as a function of time in solution with 1×10^{-2} g/L PAA.

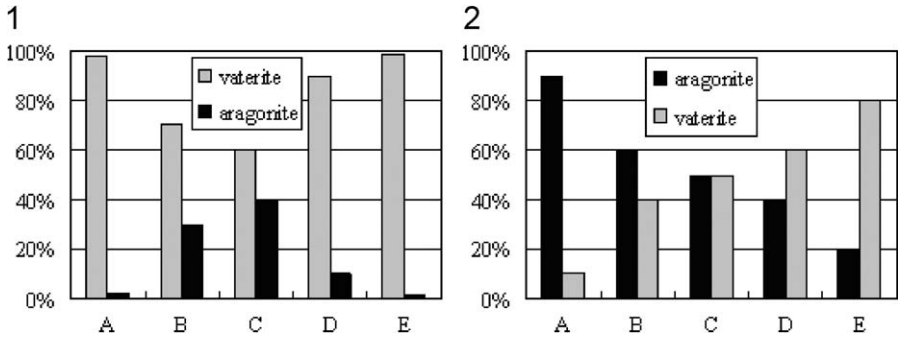

Fig. 7. The ratio of different calcium carbonate crystals grown on chitosan films (1) and acetylated chitosan films (2) in the presence of PAA: (A) 1×10^{-3} g/L; (B) 5×10^{-3} g/L; (C) 1×10^{-2} g/L; (D) 5×10^{-2} g/L; (E) 1×10^{-1} g/L.

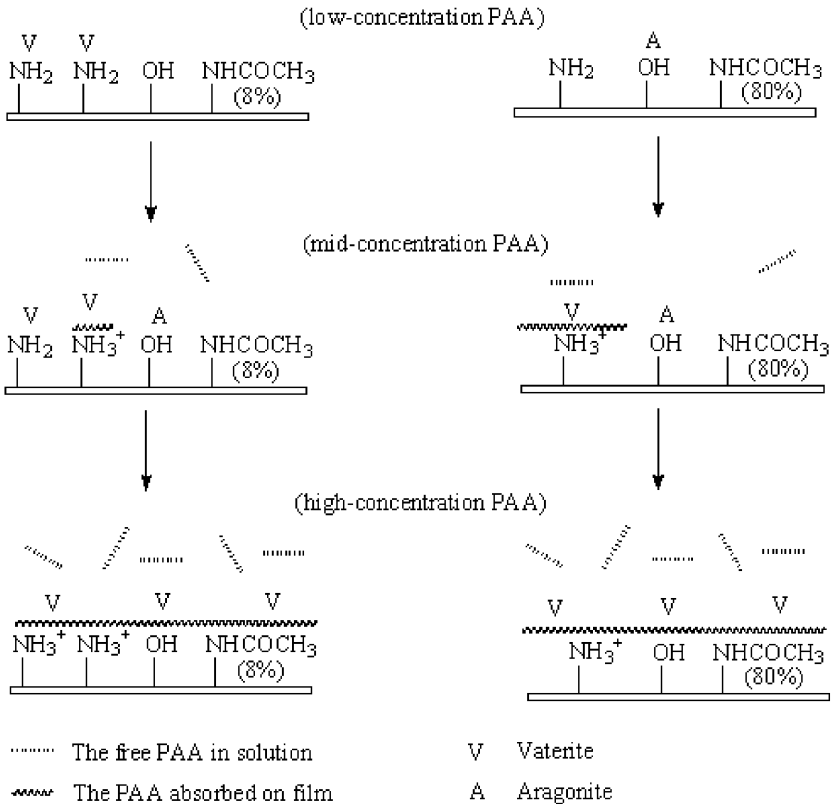

Fig. 9. Schematic presentation of the formation of calcium carbonate on chitosan films with different degrees of acetylation in the presence of PAA with low-, mid- and high concentrations (the percentages in brackets represent the ratios of $-NHCOCH_3$ in all –NH- groups).

Acknowledgment

This work was partially subsidized by Henan Innovation Project for University Prominent Research Talents (“HAIPURT”) program.

References

[1] T. Kato, A. Sugawara, N. Hosoda, Adv. Mater. 14 (2002) 869–873.
[2] T. Kato, Adv. Mater. 12 (2000) 1543–1546.
[3] S.R. Payne, M. Heppenstall-Butler, M.F. Butler, Cryst. Growth Des. 7 (2007) 1262–1267.
[4] N. Hosoda, T. Kato, Chem. Mater. 13 (2001) 688–693.
[5] S. Zhang, K.E. Gonsalves, Langmuir 14 (1998) 6761–6765.
[6] A. Kotachi, T. Miura, H. Imai, Cryst. Growth Des. 6 (2006) 1636–1642.
[7] N. Wada, S. Suda, K. Kanamura, J. Colloid Interface Sci. 279 (2004) 167–173.
[8] N. Hosoda, T. Kato, Chem. Mater. 13 (2001) 688–693.
[9] N. Hosoda, A. Sugnwara, T. Kato, Macromolecules 36 (2003) 6449–6454.
[10] P.K. Ajikumar, R. Lakshminarayanan, S. Valiyaveettil, Cryst. Growth Des. 4 (2004) 331–336.
[11] A. Berman, D.J. Ahn, A. Lio, Science 269 (1995) 515–517.
[12] G.K. Hunter, Solid State Mater. Sci. 1 (1996) 430–437.
[13] A. Jayaraman, G. Subramanyam, S. Sindu, P.K. Ajikumar, Cryst. Growth Des. 7 (2007) 142–147.
[14] A. Sugawara, A. Oichi, H. Suzuki, Y. Shigesato, J. Polym. Sci., Part A: Polym. Chem. 44 (2006) 5153–5159.
[15] F.C. Meldrum, Int. Mater. Rev. 48 (2003) 187–194.
[16] Y. Shigemasa, H. Matsuura, H. Sashiwa, Int. J. Biol. Macromol. 18 (1996) 237–244.
[17] M.L. Duarte, M.C. Ferreira, M.R. Marvao, Int. J. Biol. Macromol. 31 (2002) 1–7.
[18] J. Xu, S.P. McCarthy, R.A. Gross, Macromolecules 29 (1996) 3436–3443.
[19] A.J. Xie, C.Y. Zhang, Y.H. Shen, Cryst. Res. Technol. 41 (2006) 967–972.
[20] C. Li, G.D. Botsaris, D.L. Kaplan, Cryst. Growth Des. 2 (2002) 387–395.
[21] C.Y. Wang, J.Z. Zhao, X. Zhao, H. Bala, Powder Technol. 163 (2006) 134–140.
[22] R.C. Gifkins, Mater. Sci. Eng. C 2 (1995) 181–186.